



Calcium is associated with specific soil organic carbon decomposition products.

Mike C. Rowley^{1,2,3*}, Jasquelin Pena^{2,3*}, Matthew A. Marcus⁴, Rachel Porras², Elaine Pegoraro², Cyrill
5 Zosso^{1,5}, Nicholas O. E. Ofiti^{1,6}, Guido L. B. Wiesenberg¹, Michael W. I. Schmidt¹, Margaret S. Torn^{2,7},
& Peter S. Nico^{2,8*}.

¹Department of Geography, University of Zurich, Zurich, Switzerland.

²Earth and Environmental Sciences Area, Lawrence Berkeley National Laboratory, Berkeley, USA.

³Civil and Environmental Engineering, University of California, Davis, USA.

10 ⁴Advanced Light Source, Lawrence Berkeley National Laboratory, Berkeley, USA.

⁵Climate and Agriculture, Agroscope, Zurich, Switzerland.

⁶Institute of Ecology and Evolution, University of Bern, Bern, Switzerland.

⁷Energy and Resources Group, University of California, Berkeley, USA.

⁸Department of Environmental Science, Policy, and Management, University of California, Berkeley, USA.

15 *Correspondence to:* *mike.rowley@geo.uzh.ch.

Abstract

Calcium (Ca) may contribute to the preservation of soil organic carbon (SOC) in more ecosystems than previously thought. Here we provide evidence that Ca is co-located with SOC compounds that are enriched in aromatic and phenolic groups, across different acidic soil-types and locations with different ecosystem properties. In turn, this co-localised fraction of Ca-SOC is
20 removed through cation-exchange, and the association is then only re-established during decomposition in the presence of Ca (Ca addition incubation). Thereby highlighting a causative link between decomposition and the co-location of Ca with a characteristic fraction of SOC. Incorporating this mechanism into conceptual and numerical models can improve our



understanding, predictions, and management of carbon dynamics in natural and managed soils, and account for their response to Ca-rich amendments.

25 **Keywords**

Calcium addition, cation bridging, organo-mineral interactions, synchrotron-based spectromicroscopy, STXM C NEXAFS, Blodgett experimental forest, cation exchange, incubations.

Non-technical summary

30 This study shows calcium helps to preserve soil organic carbon in acidic soils, challenging previous beliefs that their interactions were largely limited to alkaline soils. Using spectromicroscopy, we found calcium is co-located with aromatic and phenolic-rich carbon and that this association was disrupted when the calcium was removed, and only reformed during decomposition with added calcium. This suggests that calcium amendments could enhance soil organic carbon stability.

Competing interests

The authors declare that they have no conflict of interest.



35 1.0 - Introduction

The accumulation and persistence of SOC is linked to its interactions with minerals and metal ions such as aluminium, iron (Fe), and calcium (Ca; Rasmussen et al., 2018; Kleber et al., 2021). Until recently, the effect of Ca on SOC was largely thought to be limited to soils with near-neutral to alkaline pH (Rasmussen et al., 2018; Rowley et al., 2018), or soils amended with alkaline minerals such as Ca carbonate (Paradelo et al., 2015). Yet, SOC is also co-located with Ca in carbonate-free, acidic
40 soils as confirmed recently using scanning transmission X-ray microscopy coupled with carbon (C) near-edge X-ray absorption fine structure spectroscopy (STXM C NEXAFS; Rowley et al., 2023). In the acidic grassland soils at Point Reyes, California (hereafter Grassland), Ca was co-located with SOC that contained higher proportions of aromatic- and phenolic-C, and less O-alkyl-C, relative to the SOC associated with Fe. If identified in other acidic soil environments, this could challenge our conceptual understanding that the interactions between Ca and SOC are only limited to a narrow pH range in soils (Rowley et
45 al., 2018; Rasmussen et al., 2018).

The classical model of Ca-SOC bonding involves outer-sphere cation bridging (Ca^{2+}), where Ca bridges the negatively-charged surface of a clay mineral to a SOC carboxylic functional group (Edwards and Bremner, 1967; Oades, 1988). Yet, recent studies suggest that a wider range of interactions exist between Ca and SOC, driven by an array of interacting abiotic and biotic processes (Shabtai et al., 2023; Rowley et al., 2021; Beauvois et al., 2020). It is broadly accepted that Ca can abiotically
50 influence SOC accumulation through its effects on soil aggregation and occlusion, or through different sorption processes involving various minerals or organic compounds (Fernández-Ugalde et al., 2014; Sowers et al., 2018); yet, Ca can also play an important role in decomposition of SOC and has strong effects on microbial community composition and C use efficiency (Sridhar et al., 2022b; Sridhar et al., 2022a; Schroeder et al., 2024). For instance, Shabtai et al. (2023) demonstrated that Ca addition (CaCl_2) in mesocosms shifted the microbial community towards surface-colonising organisms, which enhanced C use
55 efficiency, and decreased C mineralisation. Speculatively, these observations could imply that the co-location between Ca and a characteristic fraction of SOC in acidic grassland soils (Rowley et al., 2023) may be partly driven by microbial processes rather than physical or chemical processes alone. To confirm this hypothesis, additional STXM C NEXAFS measurements are required on both natural samples from another acidic site with different ecosystem properties, and on samples subjected to experimental treatments, including Ca removal, addition, and decomposition in the presence or absence of Ca.

60 To test the mechanism(s) underlying the association of Ca with a specific fraction of SOC, we characterised samples (plant, litter, and soil) from the Blodgett Experimental Forest (hereafter Forest), Georgetown, California, using STXM C NEXAFS and bulk chemical techniques. We then monitored the response of soils to different experiments, including cation-exchange and incubation, and compared the results to existing data from the Grassland (Rowley et al., 2023). The Forest site represents a temperate mixed-conifer site ecosystem, distinctly different from the Grassland in terms of climate, parent material, soil type,
65 and vegetation (detailed in the Methods appendix). Notably it has significantly less total Ca than the Grassland (> 20 cm depth;



Fig. S1 & S2; Table S1), thereby providing an ideal comparison for examining the association of Ca with a characteristic fraction of SOC across varied environmental conditions.

2.0 - Results and discussion

70 The STXM C K-edge NEXAFS spectra collected from acidic forest soils (pH = 3.7-6.2) show that SOC had a higher proportion of aromatic and phenolic C when co-located with Ca than with Fe (Fig. 1A & C). The C spectra of plant and litter samples from the Forest were similar irrespective of its co-location with Ca (Fig. S5); thereby, highlighting that the Ca-SOC association is not inherited from the inherent composition of plant or litter samples, but instead, seems to form in the soil. The characteristic fraction of SOC co-located with Ca in the Forest soils had a similar spectrum to that observed in the Grassland soils (Fig. S6; pH = 3.8-5.3; Rowley et al., 2023). Even though there was a large difference in total Ca content between the sites (Fig. S1 & 75 S2; Table S1), the average (total) C spectrum was only slightly closer to the Fe-C spectrum in the Forest (linear combination fitting results = 83 % Fe-C vs. 17 % Ca-C) than at the Grassland (77 % Fe-C vs. 23 % Ca-C). Cluster and non-negative matrix factorisation (NNF) analysis of the C in organo-mineral assemblages (Fig. 1B) revealed that SOC was clustered into statistically relevant groups, which were strongly associated to the distribution of Fe and Ca (Fig. 1A & B; Fig. S7). Thus, across the samples that we investigated, Ca and Fe were co-located with statistically distinct fractions of SOC, implying that 80 these elemental associations were important in dictating the distribution of SOC at the microscale (or *vice-versa*).

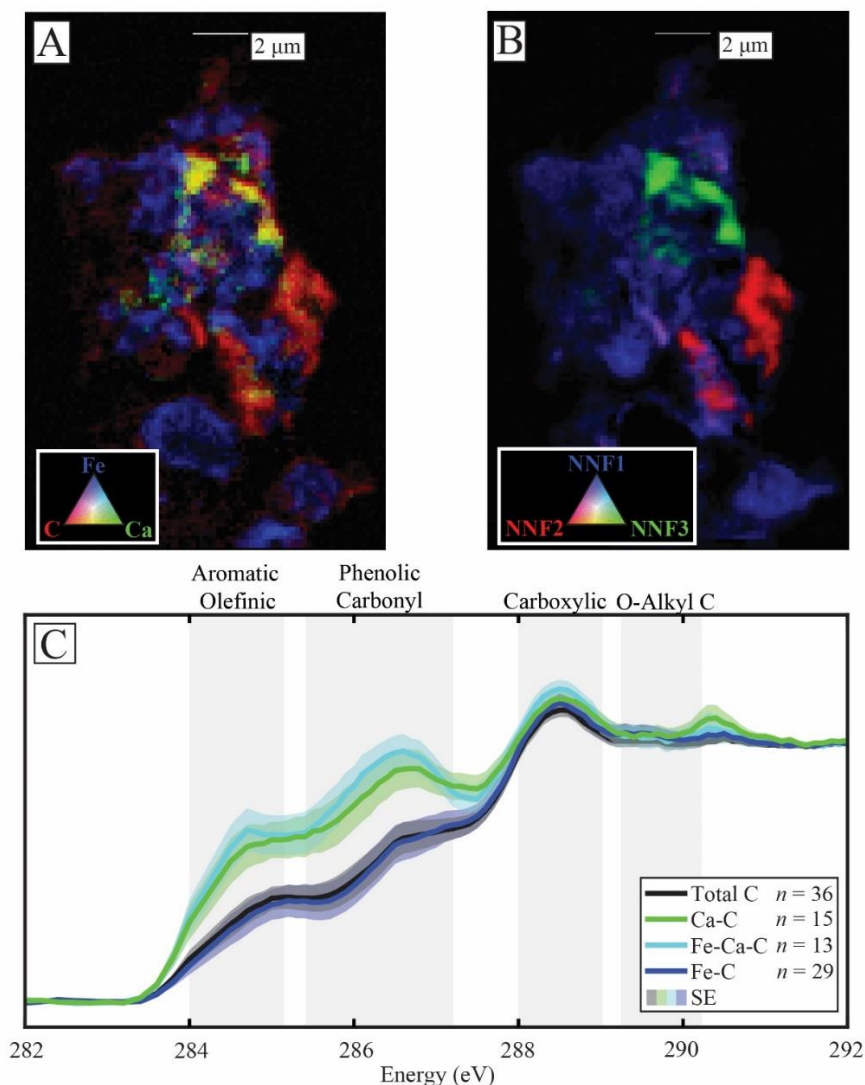


Fig. 1. The microscale co-location of Ca or iron with specific carbon compounds in soils. A.) A tricolour elemental map of the co-location of iron (blue), Ca (green), and carbon (red) in an organo-mineral assemblage from the 10-20 cm depth interval. **B.)** The fitting of non-negative matrix (NNF) factorisation statistical endmembers of carbon into clusters that correspond closely with its elemental distribution in A. The C_{1s} near-edge X-ray absorption structure spectra (NEXAFS) from these endmembers can be found in Fig. S7, in total there were 4 endmembers, but one was associated with a background signal. **C.)** The C_{1s} NEXAFS spectra of the overall carbon (total C), carbon specifically associated with only Ca (Ca-C), only iron (Fe-C), or both Ca and iron (Fe-Ca-C), with the standard error of the averaged result fitted as a shaded area outside of the spectra. Regions of the spectra associated with specific functional groups are plotted in grey behind the spectra and were attained from Lehmann et al. (2009).



To test the mechanisms governing the co-location of Ca with a characteristic fraction of SOC, we conducted two experiments. First, we conducted a potassium cation-exchange (KCl) experiment to remove the Ca from soil samples. Cation-exchange
85 leached the Ca and SOC co-located with it from our samples (Fig. 2A; Fig. S8 & S9A), lowering the aromatic and phenolic C content. This experiment confirmed that Ca preserves a characteristic fraction of SOC, preventing its export as dissolved organic C (DOC) from the Forest soils.

After this cation-exchange reaction, we re-introduced Ca to the samples, causing it to associate with soil particles and the SOC remaining after the KCl cation-exchange (Fig. 2A; Fig. S8). The STXM C NEXAFS spectra of samples post-exchange and Ca
90 addition were similar to the Fe-C spectrum, with less aromatic and phenolic C than a typical Ca-C spectrum (Fig. 1C & 2A; Fig. S9). The C pool associated with Fe was resistant to this cation-exchange procedure, suggesting that it was probably bound by inner-sphere ligand-exchange reactions. Furthermore, the composition of the C co-located with Fe supports the hypothesis that Fe oxides preferentially bind microbially-transformed SOC, rather than new plant inputs (Fig. 1C & 2A; Spielvogel et al., 2008). Contrastingly, the co-location of Ca with a characteristic fraction of SOC was irreversibly disrupted by cation-exchange
95 and, within the timeline of our experiments, could not be re-established through Ca addition alone (Fig. 2A; Fig. 7A).

In the second experiment, we incubated freshly collected soil samples after the addition of water, KCl as a control, or CaCl₂ (Fig. S4). Ca addition always reduced C mineralisation in our incubation experiments relative to the incubation with water (no
100 KCl or CaCl₂; Fig. S4; Table S2). However, in our short-term experiments, unlike Shabtai et al. (2023), we did not see a significant decrease in C mineralisation relative to the monovalent cation control (0.2 M KCl; Fig. S4; Table S2). Yet, contrasting the results of the cation-exchange experiment (Fig. 2A), one month of microbial decomposition with added Ca shifted the STXM C NEXAFS spectra of total C towards the spectra associated with Ca-C co-location (Fig. 2B; Fig. S9B). Consequently, samples that were incubated with Ca had higher aromatic and phenolic, and lower O-alkyl C, in both the Ca-C and total C spectra relative to the pre-incubation spectra (Fig. S9B). This change in the STXM C NEXAFS spectra reproduced the observations in unaltered soil samples from the Forest and Grassland (Fig. 2B; Fig. S6 & Fig. S9) suggesting it was unlikely
105 to be an artefact of the Cl⁻ addition during incubation. The decrease in O-alkyl C, indicative of labile carbohydrates, in the incubated samples instead likely resulted from microbial decomposition prior to the association of remaining fraction of SOC with Ca and its subsequent preservation. In other words, the addition of Ca during incubation led to the preservation of a characteristic fraction of SOC co-located with Ca and significantly altered overall C composition. In conclusion, the association of Ca with a characteristic fraction of SOC does not form through physicochemical mechanisms alone, but instead, arises from
110 coupled biogeochemical processes involving microbial decomposition.

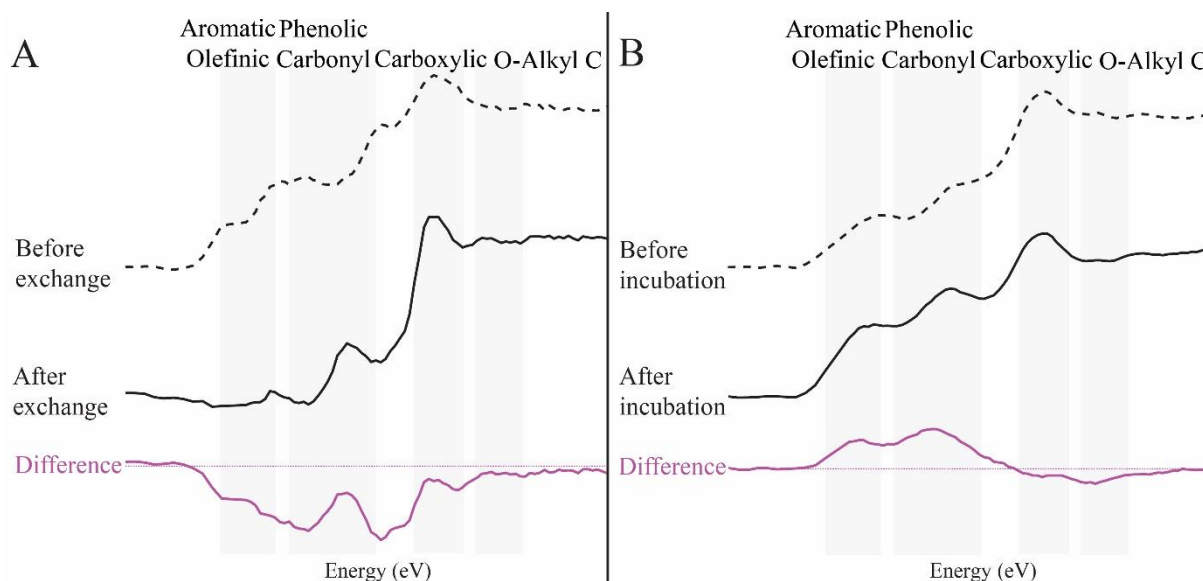


Fig. 2. Manipulation experiments demonstrate the importance of decomposition processes in the formation of the co-location of Ca with a characteristic fraction of soil organic carbon. A.) The exchange of Ca with potassium (KCl) disrupted the carbon co-located with Ca (Fig. S8), reducing the associated aromatic and phenolic carbon in the C_{1s} near-edge X-ray absorption fine structure (NEXAFS) spectra, and upon addition ($CaCl_2$), Ca re-associates with the remaining carbon (Fig. S8 & S9A). This remaining carbon has a spectrum like the carbon co-located with iron in unaltered samples (Fig. 1C), which was ultimately resistant to cation-exchange. **B.)** Incubation with added Ca reduces the O-alkyl carbon content in NEXAFS spectra while increasing the relative abundance of aromatic and phenolic carbon in the remaining sample (Fig. S9B). Thereby, microbial decomposition in the presence of added Ca reproduced a spectrum that was like the Ca-carbon spectrum of unaltered samples at the Grassland and Forest (Fig. 1C; Fig. S6). These experiments were run on two different samples from the same site explaining slight differences in the initial NEXAFS spectra, see methods for details.

The SOC fraction associated with Ca was enriched in aromatic and phenolic C, likely bound with Ca through carboxylic and hydroxyl functional groups in organo-mineral assemblages. Ca-binding affinities of C compounds at pH 4.5 do indeed increase with the number of carboxylic groups (Tam and Mccoll, 1990). The relative proportion of negatively charged functional groups increases as SOC undergoes oxidative transformation or decomposition (Lehmann and Kleber, 2015; Lehmann et al., 2020), enhancing its propensity for Ca binding (Fig. S10). We thus propose a conceptual model in which decomposition by microbes is essential as the first step for the efficient formation of Ca-SOC association. In this scenario, initial decomposition and mineralisation of O-alkyl C increases the relative proportions of Ca-binding functional groups. Upon which, this decomposed fraction can then be bound by Ca, forming its association with a characteristic fraction of SOC, protecting it in organo-mineral assemblages, inhibiting its export as DOC, and ultimately its mineralisation (Fig 2; Fig. S9).



The mechanism of co-location between Ca and a characteristic fraction of SOC was amplified by Ca addition (Fig. 2B; Shabtai et al., 2023; Sridhar et al., 2022a) and is consistently observed at the microscale across the different locations, depths, and acidic soil types. We can therefore further hypothesise that this mechanism of co-location is likely driven by Ca hotspots or abundance on the microscale, creating microdomains of decomposition that drive this characteristic association in natural samples (Kleber et al., 2021; Lehmann et al., 2020). Thus, a localised increase or microdomains in Ca availability could be driving local changes in microbial community (Shabtai et al., 2023; Sridevi et al., 2012; Sridhar et al., 2022a), decomposition pathways (Fig. 2B), the microscale distribution of C, and the association of a characteristic fraction of SOC with Ca (Fig. 1C).

This study confirms that Ca is preferentially-associated with a characteristic fraction of SOC and the formation of this co-location is driven by chemically-altered decomposition processes. Uncovering this mechanism advances our understanding of SOC decomposition and its prediction in Earth System Models. Moreover, these mechanisms of SOC retention could be enhanced through Ca-rich agricultural amendments, such as those currently applied to acidic soils as part of agricultural and climate resilience practices, in particular liming or enhanced rock weathering (Shabtai et al., 2023; Paradelo et al., 2015; Xu et al., 2024; Vicca et al., 2022). To conclude, these data show that Ca plays key roles in the cascade of biogeochemical processes that affect SOC, its decomposition, and accumulation in more environments than previously thought.

3.0 - Data availability statement

Upon publication data will be made freely available on ESS-DIVE (<https://data.ess-dive.lbl.gov/>).

4.0 - Acknowledgements

This research was based in part on material funded by the Swiss National Science Foundation (Grants P2LAP2_195077, P500PN_20665, & 200021_172744) and support to the Belowground Biogeochemistry Scientific Focus Area by the U.S. Department of Energy (DOE) Office of Science's Office of Biological and Environmental Research, Environmental Systems Science Program (under contract number DE-AC02-05CH11231). This research used resources at the Advanced Light Source, a U.S. DOE Office of Science User Facility also under contract no. DE-AC02-05CH11231. We are grateful to beamline scientists and support staff from the Advanced Light Source, including David Shapiro, David Kilcoyne, and Andrea Jones. Special thanks to Stéphanie Grand, Patricia Fox, Robert Wagner, Yves Brügger, the Peña Lab, Belowground Biogeochemistry SFA team, Deep C project, and the E.S. team, for their support with various chemical analyses, enjoyable conversations, and tours.

Appendix – Methods

Supplementary methods are also presented in the SI.



150 **Field site**

Blodgett Experimental Forest (Forest) is situated in the Sierra Nevada foothills (1370 m asl) near Georgetown, California. The Forest soils were characterised as Alfisols, which are equivalent to Dystric Cambisols (Iuss Working Group Wrb, 2015), and had formed in granitic parent materials, in a temperate climate, under thinned, mixed-coniferous forest (Fig. S3; Gaudinski et al., 2009). The results from this paper are compared to soils sampled at Point Reyes (Grassland; Fig. S3), the full description of which can be found in Rowley et al. (2023). The Grassland soils were Luvisols or Lixisols developed in mixed sedimentary deposits, in a Mediterranean climate, under mixed-grassland species (Rowley et al., 2024), which spanned an acidic pH gradient (*ca.* soil pH_{KCl} 4-5).

Sampling

Samples were taken from the whole-soil warming experiment at the Forest. This section of the research centre has been subject to whole-soil warming of +4°C since the winter of 2013, the experimental details of which can be found in Hicks Pries et al. (2017) Soil cores were sampled from the control (soil cores 1-3) and warmed (soil cores 4-6) paired plots 1-3 in May 2021 ($n = 6$), while samples for the incubations, plant (leaf and branch), and litter samples were sampled in January 2023. Samples were oven dried at 40°C, sieved to 2 mm, with a separate, adjacent soil core sampled and sent to the University of Zurich for bulk characterisation (see SI for details).

165 **Bulk characterisation.**

Soil pH was measured potentiometrically in 0.01 M Ca chloride (CaCl_2) solution at a 2:1 ratio with a Hamilton Polilyte Lab (238403) electrode. Total C and nitrogen contents were measured at the UC Davis Stable Isotope Facility using a Vario Micro Cube elemental analyser and Isoprime 100 isotope-ratio mass spectrometer. Total element contents were established using X-ray fluorescence (SPECTRO X-LAB 2000) without loss on ignition treatment.

170 **Experimental set-up**

To exchange Ca out from our samples and then add it back to the potassium-leached (exchanged) samples, we used the methods detailed in Whittinghill and Hobbie (2012). Briefly, we exchanged Ca from the soil core 4 (warmed plot 1) 60-70 cm sample using successive rinses with potassium chloride (KCl) solutions of decreasing strength ($0.1 > 0.05 > 0.01 \text{ M KCl}$), before finally washing the sample with Milli-Q H_2O ($18.2 \text{ M}\Omega \text{ cm}^{-1}$ at 25°C). To add the Ca back into the exchanged samples we resuspended the samples with 0.1 M CaCl_2 (high Ca treatment equivalent) and then rinsed with Milli-Q H_2O . Samples were centrifuged between solutions, removing the supernatant, vortexed to resuspend samples in the subsequent rinse solution, before oven drying the remaining slurry on the final rinse with H_2O at 40°C.

The incubation mesocosms were created by combining 20 g of surface soil samples from the Forest (0-20 cm) in sealed glass jars with either Milli-Q H_2O , 0.2 M KCl, or 0.1 M CaCl_2 , equivalent to $20 \text{ c.mol}_c \text{ L}^{-1}$, and then incubated at 20°C for 1 month



180 in the dark. Samples were maintained at 70 % field capacity throughout the incubation with Milli-Q H₂O. The respired CO₂
was sampled at different time points during the experiment, stored in pre-evacuated vials, replaced with Ultra Zero Air (CO₂
< 5 parts per million volume; Linde Gas and Equipment, Inc., Part # AI 0.0UZ-AS), and then measured using gas
chromatography (Shimadzu). Air was regularly replaced with Ultra Zero Air to prevent toxic concentrations of CO₂ building
up within the mesocosms, measuring and accounting for the removed CO₂. Initial SOC contents were used to calculate the
185 cumulative C respired (mg CO₂-C respired g SOC⁻¹). Pre-testing (see SI for details) revealed that Ca addition always reduced
C mineralisation in our incubation experiments relative to the incubation with water (no KCl or CaCl₂; Fig. S4; Table S2).
However, in our short-term experiments, unlike Shabtai et al. (2023), we did not see a significant decrease in C mineralisation
relative to the monovalent cation control (0.2 M KCl; Fig. S4; Table S2).

STXM C NEXAFS

190 We used STXM C NEXAFS to investigate the microscale physical and chemical association of SOC with Ca or Fe in samples
using methods detailed in Rowley et al. (2023). Briefly, soil samples from 3 depth intervals (10-20, 40-50, and 60-70 cm) of
soil cores 1-6 (control and warmed plots 1-3), plant (leaf and branch combined), litter samples from the field site, and samples
from the exchange and incubation experiments were measured at beamline 5.3.2.2 of the Advanced Light Source. We
combined observations from all plots ($n = 6$) as the exclusion of observations from the warmed plot samples (soil cores 4-6)
195 had no significant effect on the STXM C NEXAFS spectra or our interpretations. Samples were spotted onto Si₃N₄ windows
using methods adapted from Chen et al. (2014). Energy calibration was performed using CO₂ gas, setting the $1s \rightarrow 3s\sigma_g$ peak
in the C K-edge to 292.74 eV, and then checked at the end of the run (Prince et al., 1999).

Statistical and data analysis

All STXM C NEXAFS imaging and image analysis was completed in the STXM control program and C Fe STXM Image
200 Reader (Marcus, 2023), respectively. A minimum of 2 STXM C NEXAFS image stacks were collected on each sample,
background subtracted for I₀, positionally aligned, and mapped for C (295-280 eV), Ca (394.4-342 eV), and Fe (710-698 eV).
Image stacks were checked for saturation / thickness effects prior to further analysis. The image stacks were subset using a
Boolean function in C Fe STXM Image Reader to isolate the C NEXAFS spectrum corresponding to the overall C, Ca
associated C (no Fe), Fe-C (no Ca), or Fe-Ca-C signal (Rowley et al., 2023).

205 The STXM C NEXAFS stacks were investigated using principal component, clustering, and non-negative matrix factorisation
analysis to group statistically relevant endmembers or standard spectra of clustered groups of C. These endmembers were then
fit to the overall data using a least-squares fitting method. All exported spectra were background normalised in Athena (Ravel
and Newville, 2005). The edge jump was set at 284.8 eV with an intensity of 1.0, the data were normalised by fitting a second-
order polynomial to the post-edge region (291.8-302.0 eV) and the pre-edge was subtracted (279.8-283.3 eV; Rowley et al.,
210 2023). Linear combination fitting of the total C with Fe-C and Ca-C was completed in Athena (Ravel and Newville, 2005).



5.0 - References

- Beauvois, A., Vantelon, D., Jestin, J., Rivard, C., Bouhnik-Le Coz, M., Dupont, A., Briois, V., Bizien, T., Sorrentino, A., Wu, B., Appavou, M.-S., Lotfi-Kalahroodi, E., Pierson-Wickmann, A.-C., and Davranche, M.: How does calcium drive the structural organization of iron–organic matter aggregates? A multiscale investigation, *Environmental Science: Nano*, 2020. <https://doi.org/10.1039/D0EN00412J>, 2020.
- Chen, C., Dynes, J. J., Wang, J., and Sparks, D. L.: Properties of Fe-organic matter associations via coprecipitation versus adsorption, *Environmental Science & Technology*, 48, 13751-13759, <https://doi.org/10.1021/es503669u>, 2014.
- Edwards, A. P. and Bremner, J. M.: Microaggregates in soil, *Journal of Soil Science*, 18, 64, <https://doi.org/10.1111/j.1365-2389.1967.tb01488.x>, 1967.
- 215
- Fernández-Ugalde, O., Virto, I., Barré, P., Apesteguía, M., Enrique, A., Imaz, M. J., and Bescansa, P.: Mechanisms of macroaggregate stabilisation by carbonates: implications for organic matter protection in semi-arid calcareous soils, *Soil Research*, 52, 180-192, <https://doi.org/10.1071/SR13234>, 2014.
- 220
- Gaudinski, J. B., Torn, M. S., Riley, W. J., Swanston, C., Trumbore, S. E., Joslin, J. D., Majdi, H., Dawson, T. E., and Hanson, P. J.: Use of stored carbon reserves in growth of temperate tree roots and leaf buds: analyses using radiocarbon measurements and modeling, *Global Change Biology*, 15, 992-1014, <https://doi.org/10.1111/j.1365-2486.2008.01736.x>, 2009.
- 225
- Hicks Pries, C. E., Castanha, C., Porras, R. C., and Torn, M. S.: The whole-soil carbon flux in response to warming, *Science*, 355, 1420-1423, <https://doi.org/10.1126/science.aal1319>, 2017.
- IUSS Working Group WRB: World reference base for soil resources 2014, update 2015, No 106, FAO, Rome 2015.
- Kleber, M., Bourg, I. C., Coward, E. K., Hansel, C. M., Myneni, S. C. B., and Nunan, N.: Dynamic interactions at the mineral–organic matter interface, *Nature Reviews Earth & Environment*, 2, 402-421, <https://doi.org/10.1038/s43017-021-00162-y>, 2021.
- 230
- Lehmann, J. and Kleber, M.: The contentious nature of soil organic matter, *Nature*, 528, 60-68, <https://doi.org/10.1038/nature16069>, 2015.
- Lehmann, J., Solomon, D., Brandes, J., Fleckenstein, H., Jacobsen, C., and Thieme, J.: Synchrotron-based near-edge X-ray spectroscopy of natural organic matter in soils and sediments, in: *Biophysico-Chemical Processes Involving Natural Nonliving Organic Matter in Environmental Systems*, edited by: Senesi, N., Xing, B., and Huang, P. M., John Wiley & Sons Inc., Hoboken, New Jersey, 723-775, <https://doi.org/10.1002/9780470494950.ch17>, 2009.
- 235
- Lehmann, J., Hansel, C. M., Kaiser, C., Kleber, M., Maher, K., Manzoni, S., Nunan, N., Reichstein, M., Schimel, J. P., Torn, M. S., Wieder, W. R., and Kögel-Knabner, I.: Persistence of soil organic carbon caused by functional complexity, *Nature Geoscience*, 13, 529-534, <https://doi.org/10.1038/s41561-020-0612-3>, 2020.
- 240
- Marcus, M. A.: Data analysis in spectroscopic STXM, *Journal of Electron Spectroscopy and Related Phenomena*, 264, 147310, <https://doi.org/10.1016/j.elspec.2023.147310>, 2023.
- Oades, J. M.: The retention of organic matter in soils, *Biogeochemistry*, 5, 35-70, <https://doi.org/10.1007/bf02180317>, 1988.
- Paradelo, R., Virto, I., and Chenu, C.: Net effect of liming on soil organic carbon stocks: A review, *Agriculture, Ecosystems & Environment*, 202, 98-107, <https://doi.org/10.1016/j.agee.2015.01.005>, 2015.
- 245
- Prince, K. C., Avaldi, L., Coreno, M., Camilloni, R., and Simone, M. d.: Vibrational structure of core to Rydberg state excitations of carbon dioxide and dinitrogen oxide, *Journal of Physics B: Atomic, Molecular and Optical Physics*, 32, 2551-2567, <https://doi.org/10.1088/0953-4075/32/11/307>, 1999.
- Rasmussen, C., Heckman, K., Wieder, W. R., Keiluweit, M., Lawrence, C. R., Berhe, A. A., Blankinship, J. C., Crow, S. E., Druhan, J. L., Hicks Pries, C. E., Marin-Spiotta, E., Plante, A. F., Schädel, C., Schimel, J. P., Sierra, C. A., Thompson, A., and Wagai, R.: Beyond clay: towards an improved set of variables for predicting soil organic matter content, *Biogeochemistry*, 137, 297-306, <https://doi.org/10.1007/s10533-018-0424-3>, 2018.
- 250
- Ravel, B. and Newville, M.: ATHENA, ARTEMIS, HEPHAESTUS: Data analysis for X-ray absorption spectroscopy using IFEFFIT. [code], 2005.
- 255
- Rowley, M. C., Grand, S., and Verrecchia, E. P.: Calcium-mediated stabilisation of soil organic carbon, *Biogeochemistry*, 137, 27-49, <https://doi.org/10.1007/s10533-017-0410-1>, 2018.
- Rowley, M. C., Grand, S., Spangenberg, J. E., and Verrecchia, E. P.: Evidence linking calcium to increased organo-mineral association in soils, *Biogeochemistry*, 153, 223-241, <https://doi.org/10.1007/s10533-021-00779-7>, 2021.



- 260 Rowley, M. C., Falco, N., Pegoraro, E., Dafflon, B., Gerlein-Safdi, C., Wu, Y., Castanha, C., Peña, J., Nico, P. S., and Torn, M. S.: The importance of accounting for landscape position when investigating grasslands: A multidisciplinary characterisation of a California coastal grassland, *Earth's Future*, 12, 1-20, <https://doi.org/10.1029/2023EF004208>, 2024.
- Rowley, M. C., Nico, P. S., Bone, S. E., Marcus, M. A., Pegoraro, E. F., Castanha, C., Kang, K., Bhattacharyya, A., Torn, M. S., and Peña, J.: Association between soil organic carbon and calcium in acidic grassland soils from Point Reyes National Seashore, CA, *Biogeochemistry*, 165, 91-111, <https://doi.org/10.1007/s10533-023-01059-2>, 2023.
- 265 Schroeder, J., Dămătîrcă, C., Bölscher, T., Chenu, C., Elsgaard, L., Tebbe, C. C., Skadell, L., and Poeplau, C.: Liming effects on microbial carbon use efficiency and its potential consequences for soil organic carbon stocks, *Soil Biology and Biochemistry*, 191, 1-20, <https://doi.org/10.1016/j.soilbio.2024.109342>, 2024.
- Shabtai, I. A., Wilhelm, R. C., Schweizer, S. A., Höschen, C., Buckley, D. H., and Lehmann, J.: Calcium promotes persistent soil organic matter by altering microbial transformation of plant litter, *Nature Communications*, 14, 6609-6622, <https://doi.org/10.1038/s41467-023-42291-6>, 2023.
- 270 Sowers, T. D., Stuckey, J. W., and Sparks, D. L.: The synergistic effect of calcium on organic carbon sequestration to ferrihydrite, *Geochemical Transactions*, 19, 4, <https://doi.org/10.1186/s12932-018-0049-4>, 2018.
- Spielvogel, S., Prieszel, J., and Kögel-Knabner, I.: Soil organic matter stabilization in acidic forest soils is preferential and soil type-specific, *European Journal of Soil Science*, 59, 674-692, <https://doi.org/10.1111/j.1365-2389.2008.01030.x>, 2008.
- 275 Sridevi, G., Minocha, R., Turlapati, S. A., Goldfarb, K. C., Brodie, E. L., Tisa, L. S., and Minocha, S. C.: Soil bacterial communities of a calcium-supplemented and a reference watershed at the Hubbard Brook Experimental Forest (HBEF), New Hampshire, USA, *FEMS Microbiology Ecology*, 79, 728-740, <https://doi.org/10.1111/j.1574-6941.2011.01258.x>, 2012.
- Sridhar, B., Wilhelm, R. C., Debenport, S. J., Fahey, T. J., Buckley, D. H., and Goodale, C. L.: Microbial community shifts correspond with suppression of decomposition 25 years after liming of acidic forest soils, *Global Change Biology*, 28, 5399-5415, <https://doi.org/10.1111/gcb.16321>, 2022a.
- 280 Sridhar, B., Lawrence, G. B., Debenport, S. J., Fahey, T. J., Buckley, D. H., Wilhelm, R. C., and Goodale, C. L.: Watershed-scale liming reveals the short- and long-term effects of pH on the forest soil microbiome and carbon cycling, *Environmental Microbiology*, 24, 6184-6199, <https://doi.org/10.1111/1462-2920.16119>, 2022b.
- Tam, S.-C. and McColl, J. G.: Aluminum- and calcium-binding affinities of some organic ligands in acidic conditions, *Journal of Environmental Quality*, 19, 514-520, <https://doi.org/10.2134/jeq1990.00472425001900030027x>, 1990.
- 285 Vicca, S., Goll, D. S., Hagens, M., Hartmann, J., Janssens, I. A., Neubeck, A., Peñuelas, J., Poblador, S., Rijnders, J., Sardans, J., Struyf, E., Swoboda, P., van Groenigen, J. W., Vienne, A., and Verbruggen, E.: Is the climate change mitigation effect of enhanced silicate weathering governed by biological processes?, *Global Change Biology*, 28, 711-726, <https://doi.org/10.1111/gcb.15993>, 2022.
- 290 Whittinghill, K. A. and Hobbie, S. E.: Effects of pH and calcium on soil organic matter dynamics in Alaskan tundra, *Biogeochemistry*, 111, 569-581, <https://doi.org/10.1007/s10533-011-9688-6>, 2012.
- Xu, T., Yuan, Z., Vicca, S., Goll, D. S., Li, G., Lin, L., Chen, H., Bi, B., Chen, Q., Li, C., Wang, X., Wang, C., Hao, Z., Fang, Y., and Beerling, D. J.: Enhanced silicate weathering accelerates forest carbon sequestration by stimulating the soil mineral carbon pump, *Global Change Biology*, 30, 1-17, <https://doi.org/10.1111/gcb.17464>, 2024.

295